Copy 6
RM E55B25

NACA RM E55B25

RESEARCH MEMORANDUM

EFFECT ON EJECTOR PERFORMANCE OF VARYING DIAMETER RATIO BY SIMULATED IRIS FLAPS

By Alfred S. Valerino and Leonard E. Stitt

Lewis Flight Propulsion Laboratory
Cleveland, Ohio

NATIONAL ADVISORY COMMITTEE
FOR AERONAUTICS

WASHINGTON
April 21, 1955

NACA RM E55B25

NATIONAL ADVISORY COMMITTEE FOR AERONAUTICS

RESEARCH MEMORANDUM

EFFECT ON EJECTOR PERFORMANCE OF VARYING DIAMETER RATIO BY SIMULATED IRIS FLAPS

By Alfred S. Valerino and Leonard E. Stitt

SUMMARY

An investigation was conducted in the NACA Lewis 8- by 6-foot supersonic wind tunnel at free-stream Mach numbers of 0.10, 0.63, and 1.50 for a range of primary-nozzle pressure ratios and secondary weight-flow ratios to determine the effects on performance of varying the ejector diameter ratio by simulated iris flaps. Primary gas temperatures from 1000° to 2000° R were obtained by combustion of gasoline in the primary stream.

Results of the investigation indicated that increases in both ejector gross force and secondary-to-primary total-pressure ratio were obtained subsonically when the diameter ratio was reduced from 1.54 to 1.17, thus reducing overexpansion losses. At a free-stream Mach number of 1.5, reducing the diameter ratio to 1.17 resulted in an increase in ejector gross force only at the low secondary weight flows. At high secondary weight-flow ratios, the large-diameter-ratio ejector yielded the highest gross force.

INTRODUCTION

In order to obtain maximum thrust, an engine which operates with and without an afterburner over a wide range of flight speeds requires an exhaust nozzle in which the expansion ratio as well as the throat area is variable. These area variations should be independent for optimum thrust performance. One method for independent control of expansion ratio is the use of an ejector nozzle with a variable shroud diameter (varied by means of iris-type flaps) as well as a primary-nozzle diameter.

The present investigation was part of an over-all study that was conducted in the Lewis 8- by 6-foot supersonic tunnel to evaluate the performance of a series of ejectors at subsonic and supersonic flight speeds. References 1 and 2 report the performance with the primary nozzle in the simulated afterburner-on and afterburner-off positions and

with the shroud diameter set at large values corresponding to high-pressure-ratio operation with the afterburner on. This report presents the experimental gross-force and pumping characteristics of a series of ejectors in which the primary nozzle was in the afterburner-off position but where the diameter ratio of the ejector was varied by simulated iris-flap configurations on the afterbody shroud.

The investigation was conducted at free-stream Mach numbers of 0.10, 0.63, and 1.50 over a range of primary-nozzle pressure ratios and secondary weight flows. The temperature of the gas through the primary nozzle varied from 1000° to 2000° R.

SYMBOLS

The following symbols are used in this report and some are shown in the following sketch:

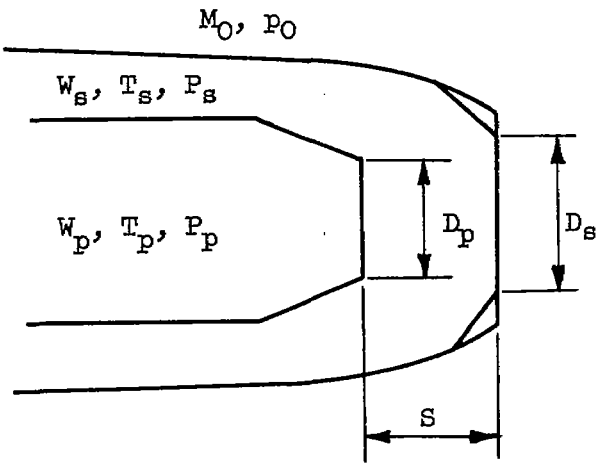

A	area, sq in.
C_f	discharge coefficient, ratio of measured mass flow to isentropic one-dimensional mass flow
D	exit diameter, in.
D_s/D_p	diameter ratio
d	drag
F	thrust or force, lb
M	Mach number

P	total pressure, lb/sq ft
P_p/p_0	pressure ratio, ratio of total to free-stream static pressure
p	static pressure, lb/sq ft
S	spacing, distance from primary-nozzle exit to shroud exit, in.
S/D_p	spacing ratio
T	total temperature, $^\circ R$
W	weight flow, lb/sec
$\frac{W_s}{W_p}\sqrt{\frac{T_s}{T_p}}$	corrected weight-flow ratio
γ	ratio of specific heats

Subscripts:

a	boattail
e	ejector
j	jet
p	primary nozzle
s	secondary passage
0	free stream

APPARATUS AND PROCEDURE

Installation. - The model installation in the Lewis 8- by 6-foot supersonic wind tunnel is shown by the schematic drawing and photograph in figures 1(a) and (b), respectively. Air, which was preheated to 250° F, was introduced into the model through two hollow support struts. A detailed discussion of the model installation in the tunnel is presented in reference 3. The temperature of the gas through the primary nozzle was varied from 1000° to 2000° R by a gasoline combustor ahead of the nozzle (see ref. 1). A schematic diagram of the model showing pertinent external model stations and internal details is presented in figure 2. The external shrouds investigated were mounted at station 70.61.

[redacted]

Ejector configurations. - Sketches and pertinent dimensions of the ejectors investigated are presented in figure 3 together with tables of internal contour coordinates of the shrouds. The primary nozzle, which was the same for all the shroud configurations investigated, had a throat diameter of 2.82 inches simulating the afterburner-off case. The collar around the primary nozzle simulated a portion of an actual nozzle control mechanism. The ejector configurations are designated either by two numbers or by two numbers followed by one or two letters; the first number indicates the diameter ratio D_s/D_p; the second number indicates the spacing ratio S/D_p. When the two numbers are followed by the letters I or SI, the ejector utilizes iris or shrouded iris flaps. Shrouded iris flaps alter the internal contour of the extended shroud but not the external contour.

The ejector configurations investigated were developed from a basic configuration having a diameter ratio of 1.97 and a spacing ratio of zero (fig. 3(a)). The shroud was extended as would be necessary for satisfactory afterburner-on performance at a design flight Mach number of 1.9. In these studies, with the afterburner off, this extended shroud configuration has a diameter ratio of 1.54 and a spacing ratio of 1.11 (fig. 3(b)). To decrease the jet overexpansion at the lower primary-nozzle pressure ratios, the diameter ratio was decreased to 1.35 and 1.17 while maintaining approximately the same spacing ratio by use of simulated iris and shrouded iris flaps (figs. 3(c) to (f)). It should be noted that the flap angularities of the shrouded iris-flap configurations differ from those of the iris-flap configurations.

Data reduction. - The method of force measurements and the reduction of these data are described in reference 1. Model total weight flow was obtained from the sharp-edged orifice shown in figure 1(a) and from rotameters that measured preheater and main combustor fuel flow. Primary-nozzle weight flow W_p was calculated by subtracting the calibrated secondary weight flow W_s from the total weight flow. Primary-nozzle total pressure was obtained from the static pressure measured at station 70.16 and the Mach number determined from the nozzle-area ratio and the nozzle discharge coefficient C_f. The nozzle discharge coefficient, defined as the ratio of actual to ideal weight flow, was determined experimentally with preheated air only. Primary-nozzle total temperature was obtained from continuity relations where total pressure, weight flow, and discharge coefficient were known.

Boattail drags of ejector 1.35-1.11SI were calculated by an integration of boattail static pressures obtained from eight static orifices shown in figure 3(c). The shrouded flap drags of ejector 1.17-1.11SI were evaluated from four static orifices located on the flaps as shown in figure 3(e).

RESULTS AND DISCUSSION

Ejector Performance

Presented in figure 4 for free-stream Mach numbers M_0 of 0.1, 0.63, and 1.50 are the ratios of ejector secondary-to-primary total pressure and ejector gross force as a function of corrected weight-flow ratio for constant values of primary-nozzle pressure ratio. The gross ejector force is presented as a function of the jet thrust of the primary nozzle $F_{j,p}$, determined experimentally at jet stream temperatures of 1000° to 2000° R, and shown in figure 5. The ejector gross force is defined as the sum of the measured thrust minus drag and the jet-off external drag of ejector 1.97-0. The gross force thus includes the ejector jet thrust plus any difference in external afterbody drag between the experimental ejector and the reference ejector 1.97-0. Although these data cannot be directly compared with ejector internal thrust data, a relative comparison of configurations is permitted.

To facilitate the comparison of configurations, the experimental data of figure 4 were used to obtain the cross plots of secondary-to-primary total-pressure ratio and gross-force ratio as a function of nozzle pressure ratio presented in figure 6. Data points are shown only to distinguish free-stream Mach number since the curves represent interpolated values. On each of the curves of figure 6, the value of primary-nozzle pressure ratio supplied by a typical present day engine is indicated for each of the three values of free-stream Mach number.

A downward shift of gross-force ratio occurred for a change in Mach number from subsonic values to a supersonic value of 1.50. This shift resulted from decreases in the local static pressures on the boattail and in the secondary-passage regions associated with the supersonic external stream expansion. Gross-force ratio increased with increasing secondary weight flow because of the reduction of jet overexpansion losses. Increases in secondary weight flow also decreased the downward shift in the gross-force-ratio curves resulting from the Mach number change from 0.63 to 1.5. This decrease in downward shift was less pronounced for the small-diameter-ratio flap configurations.

Figure 7 presents the variation of ejector gross-force ratio and pumping characteristics as a function of free-stream Mach number. These data were obtained from figure 6 for the values of nozzle pressure ratio corresponding to a typical engine operating schedule. Since the primary-nozzle pressure ratios are relatively low at subsonic speeds (P_p/p_0 equal to 2.5 and 3.4 at free-stream Mach numbers of 0.10 and 0.63, respectively), the jet is increasingly overexpanded as diameter ratio is increased. As a result, the ejector gross-force ratios of the high-diameter-ratio ejectors are low, while the ejectors having the lower diameter ratio of 1.17 had a higher gross-force ratio. At the supersonic

Mach number of 1.5, the ejector gross force of the large-diameter-ratio ejector remained low for small secondary weight flows since the potential improvement due to increased pressure ratio was nullified by the adverse stream effects discussed previously and in reference 2. Increase in secondary weight flow improved the ejector gross force by decreasing overexpansion in the ejector and by reducing the adverse external stream effects.

An increase in free-stream Mach number from 0.63 to 1.5 with ejector 1.17-1.00I resulted in a reduction in gross-force ratio at all values of secondary weight flow. This reduction was due to the increase in base or boattail drag. At a free-stream Mach number of 1.5, up to and including the secondary weight-flow ratio of 0.15, ejector 1.17-1.00I was superior on a gross-force basis over the other ejectors investigated since it is more nearly sized properly for the available pressure ratio P_p/p_0. When the secondary weight-flow ratio was increased to over 0.15, the superiority of ejector 1.17-1.00I over the other ejectors was marginal. This marginal superiority was in part caused by the decrease in the primary-nozzle jet thrust of the small-diameter-ratio ejector (associated with the decrease in primary-nozzle discharge-flow coefficients at high secondary weight flows, ref. 1) and in part by the improvement in performance of the large-diameter-ratio ejectors.

The effect of reducing diameter ratio on the performance of the ejectors is summarized in figure 8. For subsonic external flow, decreases in diameter ratio resulted in an increase in gross force over that of ejector 1.54-1.11. This gain in gross force increased with increasing secondary flow. The iris-flap configurations generally exhibited gross-force characteristics slightly superior to the shrouded iris-flap configurations. At a Mach number of 1.5 and at low secondary weight flows, ejector 1.17-1.00I again yielded the highest gross force. At these low weight-flow ratios, the gross force of ejectors 1.35-1.11SI and 1.54-1.11 were comparable. When the secondary weight-flow ratio was increased to 0.35, highest gross force was obtained with the largest-diameter-ratio ejector, 1.54-1.11.

Boattail Drag

Some indication of the magnitude of the boattail drag of ejector 1.35-1.11SI is obtained from figure 9 where the drag is presented as a percentage of the measured primary-nozzle jet thrust. In general, for a given value of free-stream Mach number, the boattail drag ratio decreased with increasing values of both secondary weight flow and primary-nozzle pressure ratio (ref. 4). The boattail drag ratio increased as free-stream Mach number was increased. At a Mach number of 1.5 and at a typical nozzle operating point ($P_p/p_0 = 6.7$), the maximum boattail drag corresponded to approximately 8 percent of the nozzle jet thrust. At subsonic speeds, however, the boattail drag was relatively low in value.

Shrouded Iris-Flap Force

The flap force computed for ejector 1.17-1.11SI is presented in figure 10. Drag forces were obtained at Mach numbers of 0.10 and 1.5. However, at Mach number 0.63, a small thrust force was obtained. The flap force reached a maximum of 5 percent of the primary-nozzle thrust at Mach number 1.5 for a pressure ratio of 4.75.

SUMMARY OF RESULTS

An investigation was conducted in the Lewis 8- by 6-foot supersonic tunnel to determine the effect on ejector performance of varying diameter ratio by simulated iris flaps. The investigation was conducted at Mach numbers of 0.10, 0.63, and 1.50 over a range of primary pressure and secondary weight-flow ratios. The following results were obtained:

1. At subsonic speeds, reducing the ejector diameter ratio from excessively large values by either the iris or shrouded iris flaps generally resulted in increases in ejector gross force and secondary-to-primary total-pressure ratios.

2. At a free-stream Mach number of 1.5, an increase in gross force was obtained at low values of secondary weight-flow ratio by decreasing the ejector diameter ratio from 1.54 to 1.17. At very high values of secondary weight-flow ratio (0.35), the best gross-force performance was obtained with the large-diameter-ratio ejector.

Lewis Flight Propulsion Laboratory
National Advisory Committee for Aeronautics
Cleveland, Ohio, March 1, 1955

REFERENCES

1. Hearth, Donald P., and Valerino, Alfred S.: Thrust and Pumping Characteristics of a Series of Ejector-Type Exhaust Nozzles at Subsonic and Supersonic Flight Speeds. NACA RM E54H19, 1954.

2. Stitt, Leonard E., and Valerino, Alfred S.: Effect of Free-Stream Mach Number on Gross-Force and Pumping Characteristics of Several Ejectors. NACA RM E54K23a, 1955.

3. Hearth, Donald P., and Gorton, Gerald C.: Investigation of Thrust and Drag Characteristics of a Plug-Type Exhaust Nozzle. NACA RM E53L16, 1954.

4. Gorton, Gerald C.: Pumping and Drag Characteristics of an Aircraft Ejector at Subsonic and Supersonic Speeds. NACA RM E54D06, 1954.

[redacted]

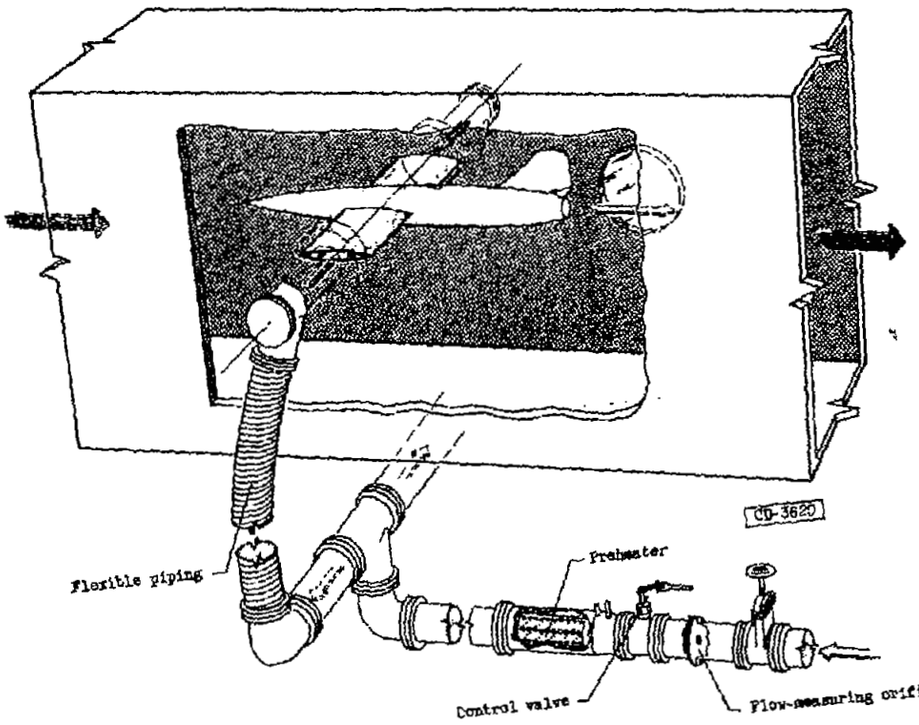

(a) Schematic diagram.

Figure 1.- Model installation in Lewis 8- by 6-foot supersonic wind tunnel.

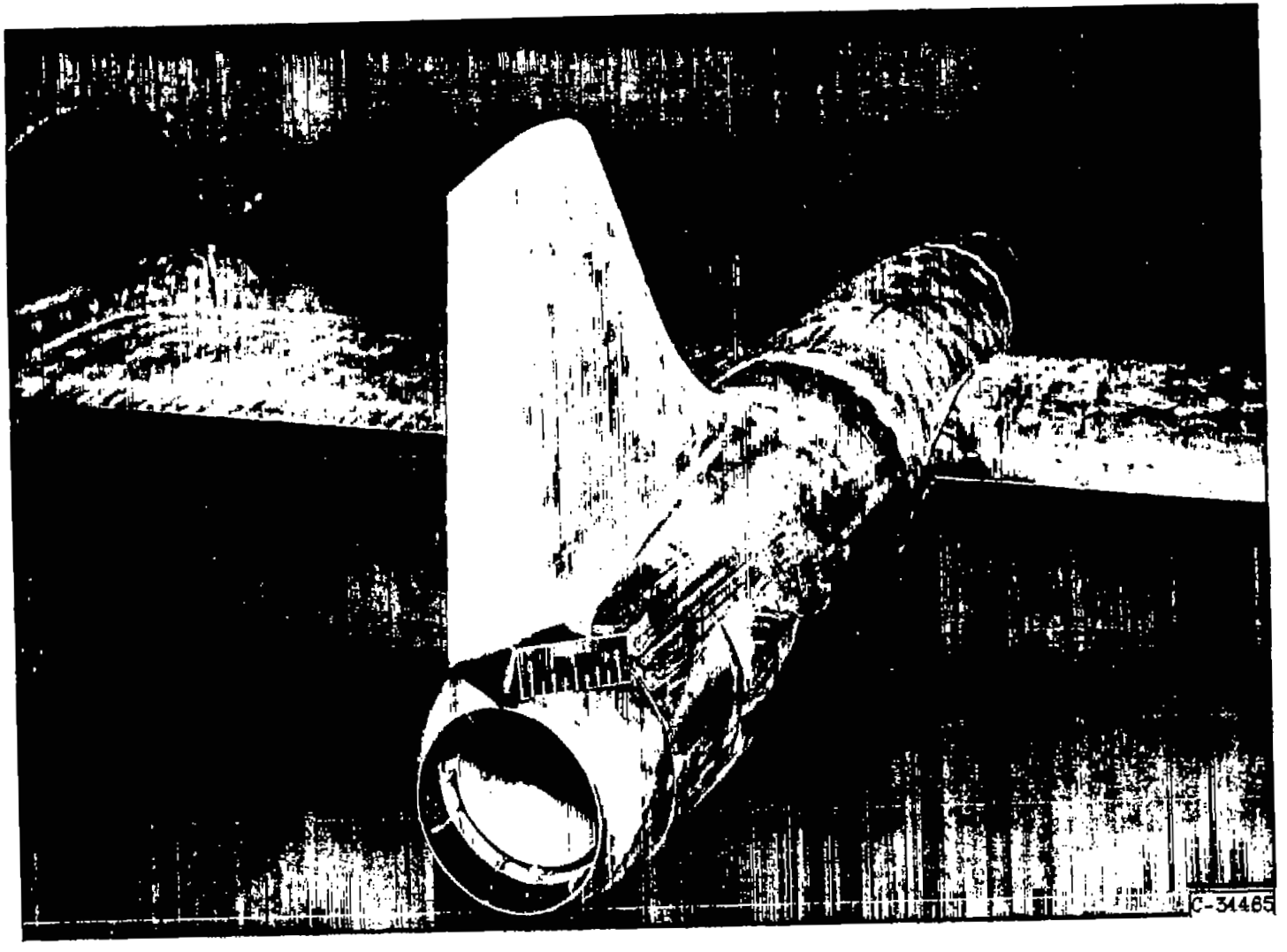

(b) Photograph of typical model without iris-flap modification.

Figure 1.- Concluded. Model installation in 8- by 6-foot supersonic wind tunnel.

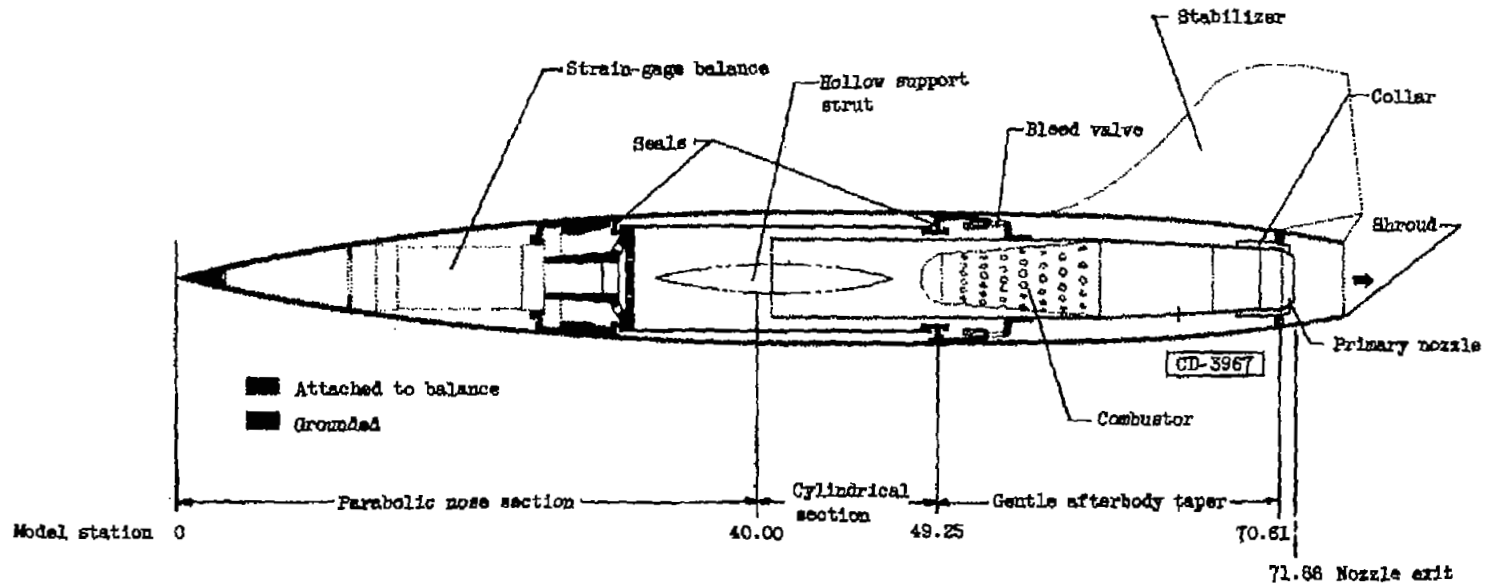

Figure 2. - Schematic diagram of model. (All dimensions in inches.)

Shroud internal contour	
Fuselage station	Inside diameter, in.
70.61	5.74
71.66	5.55

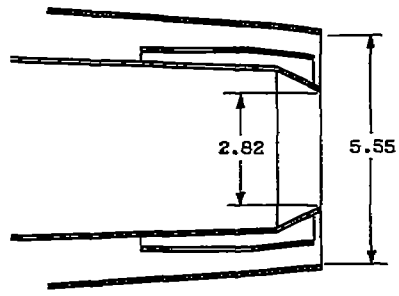

(a) Ejector 1.97-0.

Shroud internal contour	
Fuselage station	Inside diameter, in.
70.61	5.74
71.66	5.55
72.72	5.26
73.77	4.86
74.79	4.34

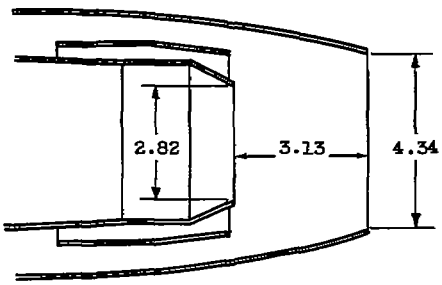

(b) Ejector 1.54-1.11.

Shroud internal contour	
Fuselage station	Inside diameter, in.
70.61	5.74
71.66	5.55
72.72	5.26
73.77	4.74
74.79	3.82

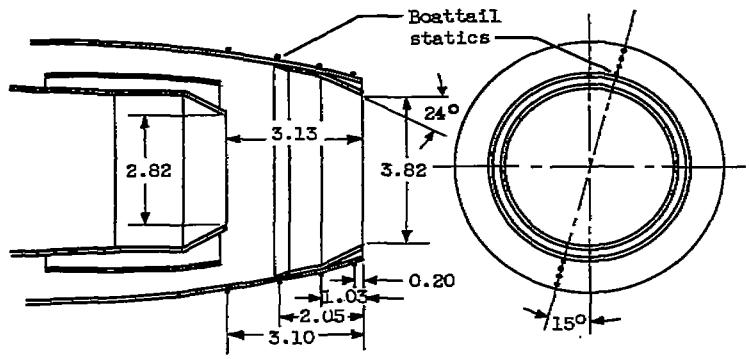

(c) Ejector 1.35-1.11SI.

Figure 3. - Ejector configurations. (All dimensions in inches.)

Shroud internal contour	
Fuselage station	Inside diameter, in.
70.61	5.74
71.66	5.55
72.72	5.26
73.77	4.86
74.64	3.82

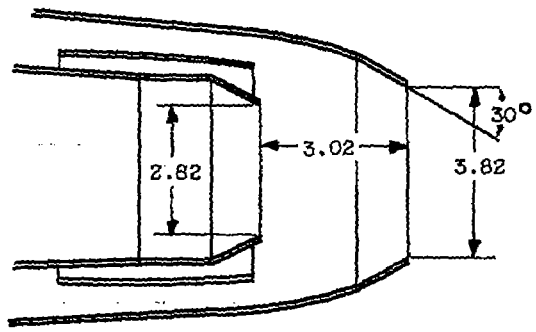

(d) Ejector 1.35-1.07 I.

Shroud internal contour	
Fuselage station	Inside diameter, in.
70.61	5.74
71.66	5.55
72.72	5.26
73.77	4.74
74.79	3.31

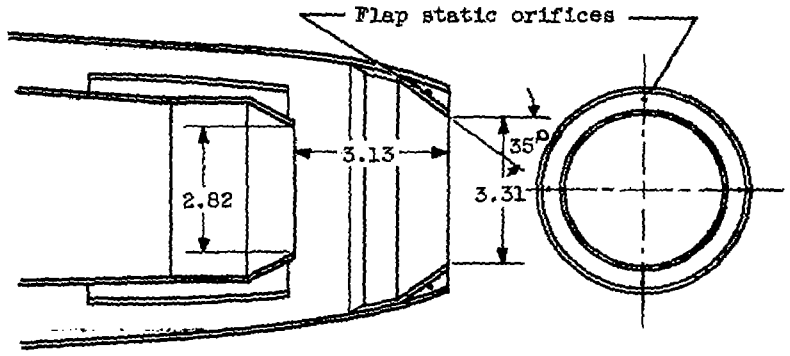

(e) Ejector 1.17-1.11 SI.

Shroud internal contour	
Fuselage station	Inside diameter, in.
70.61	5.74
71.66	5.55
72.72	5.26
73.77	4.86
74.43	3.31

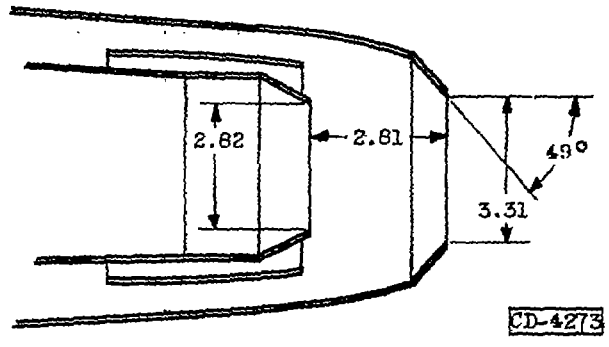

(f) Ejector 1.17-1.00 I.

Figure 3. -Concluded. Ejector configurations. (All dimensions in inches.)

[redacted]

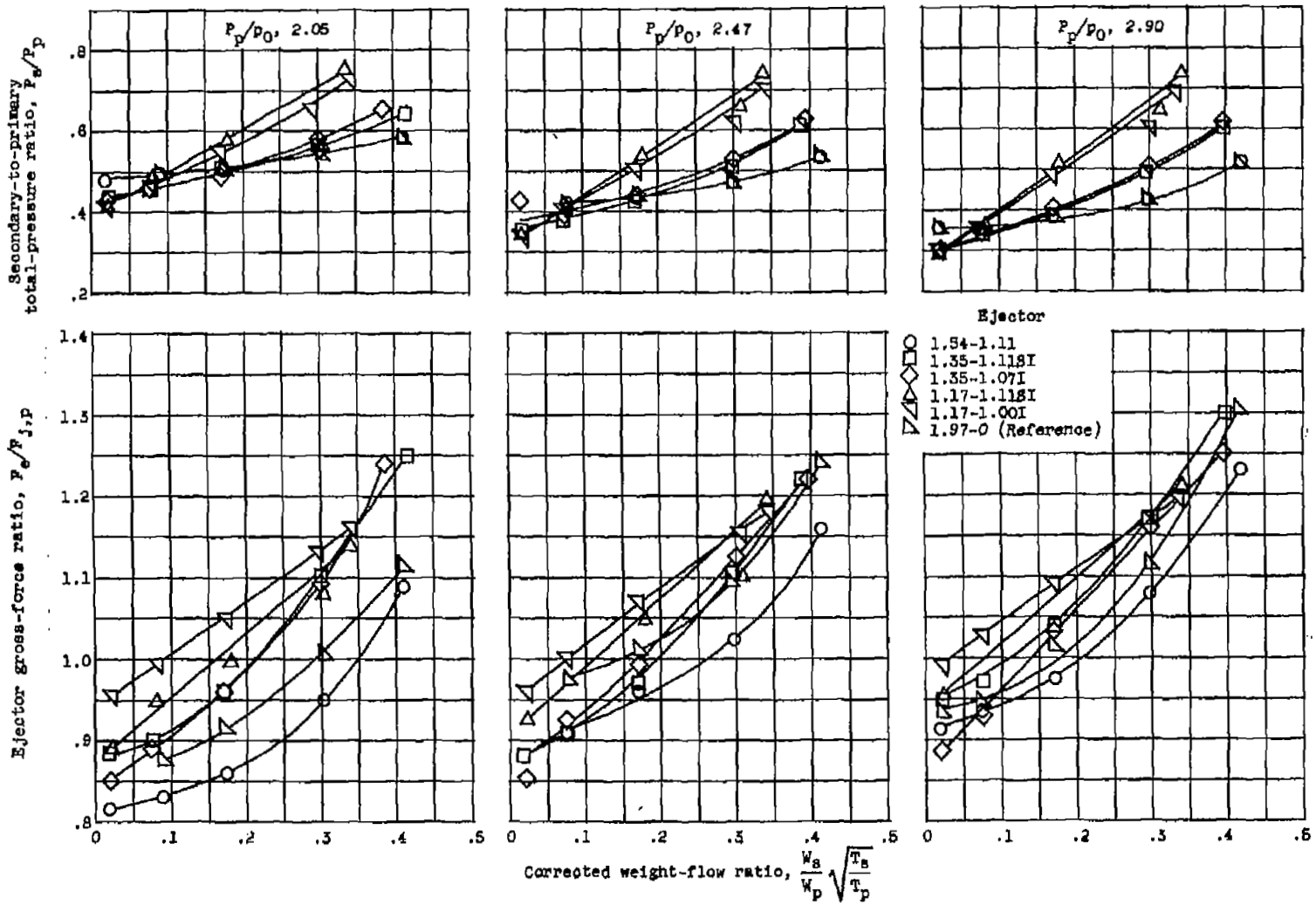

(a) Free-stream Mach number, 0.10.

Figure 4. - Ejector pumping and gross-force characteristics.

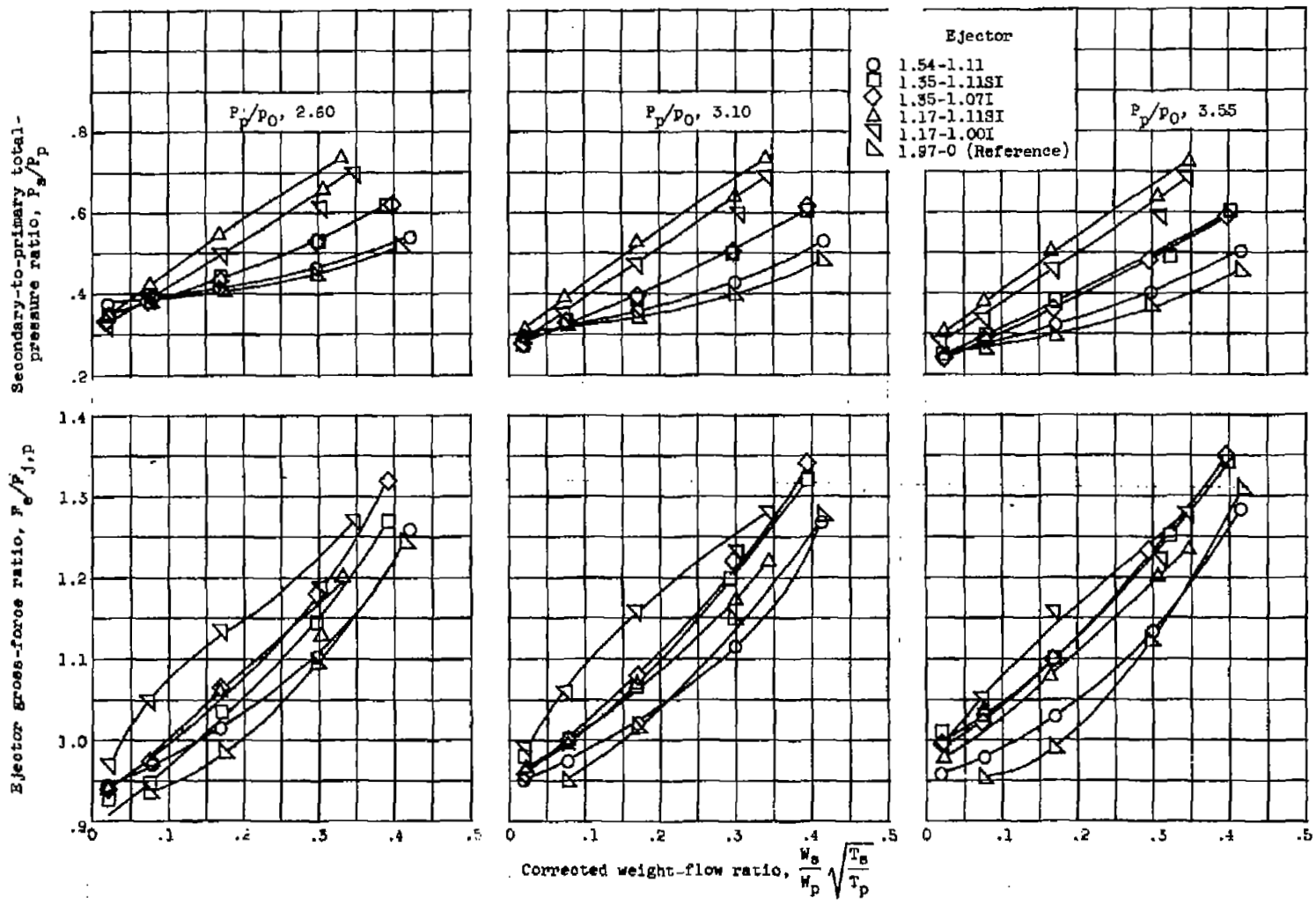

(b) Free-stream Mach number, 0.63.

Figure 4. - Continued. Ejector pumping and gross-force characteristics.

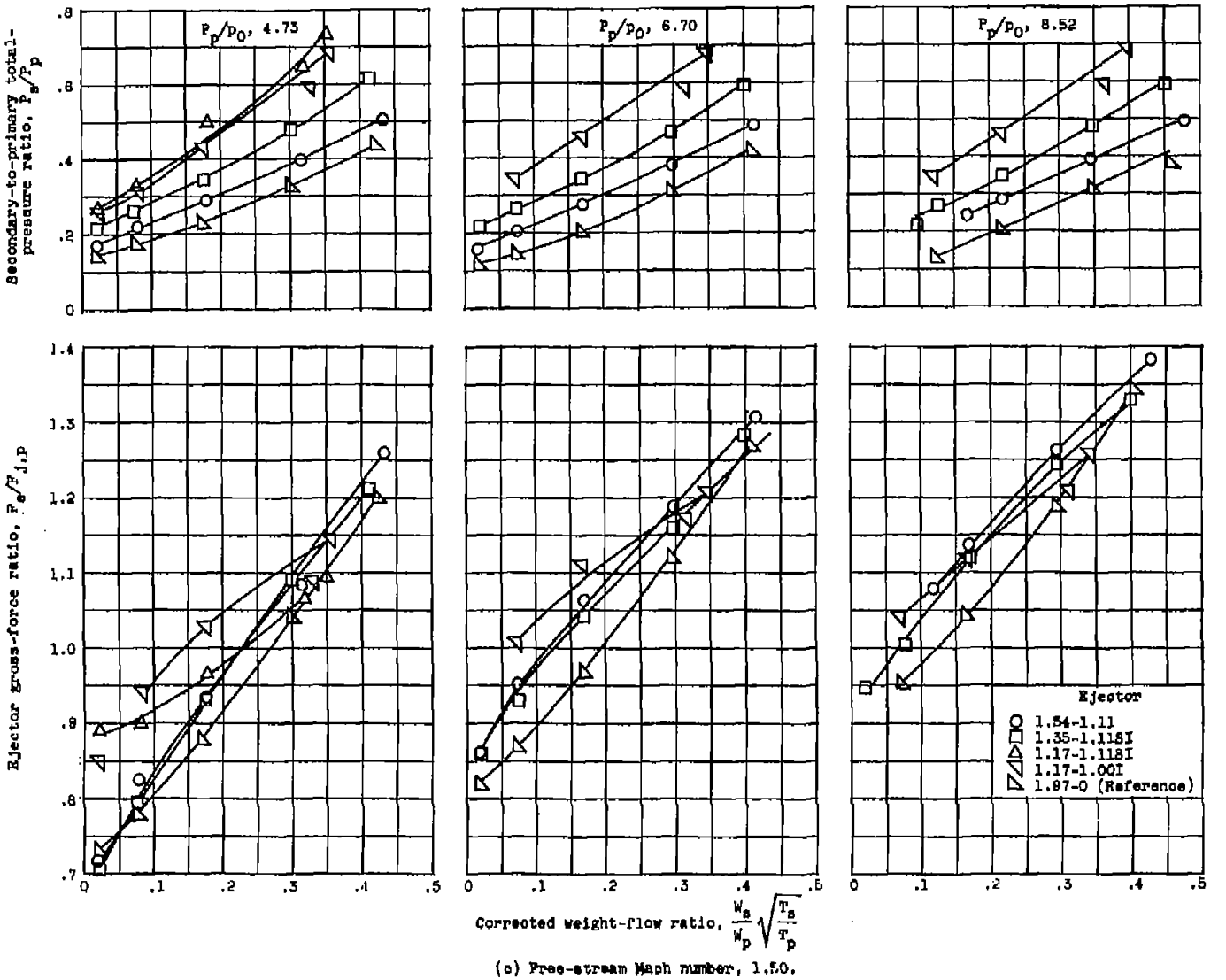

(c) Free-stream Mach number, 1.50.

Figure 4. - Concluded. Ejector pumping and gross-force characteristics.

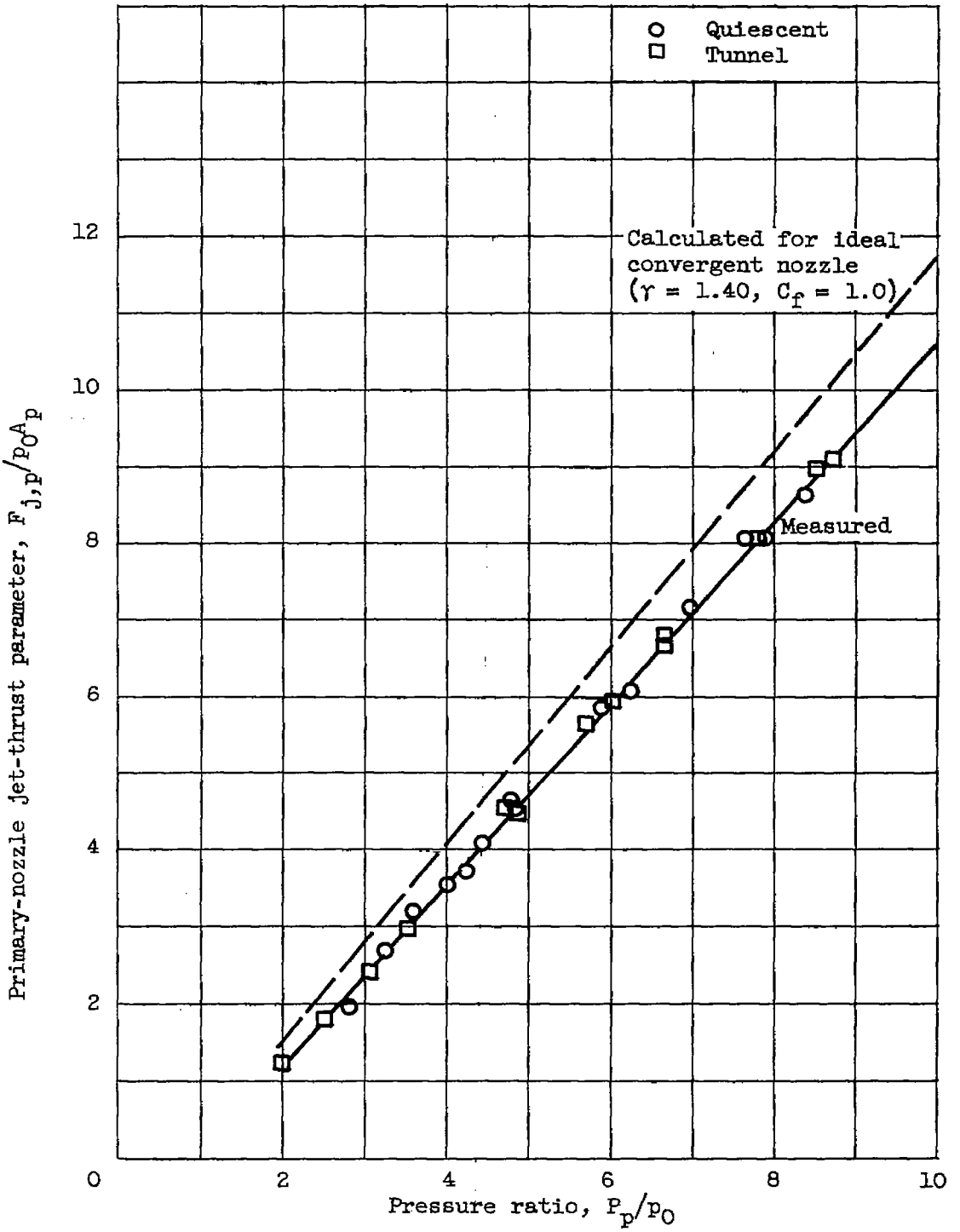

Figure 5. - Jet-thrust performance of 2.82-inch-diameter conical primary nozzle.

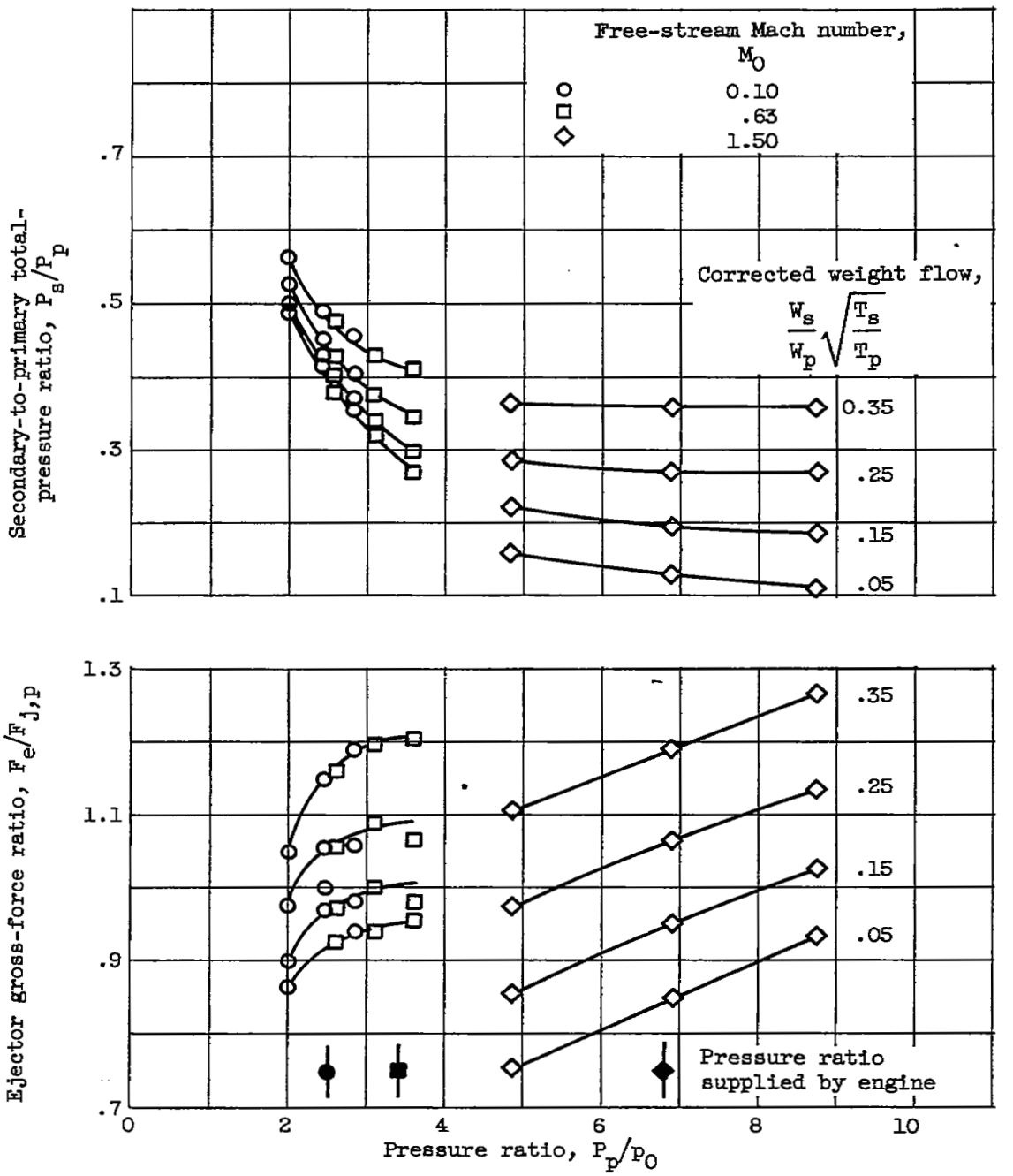

(a) Ejector 1.97-0 (reference configuration).

Figure 6. - Effect of primary-nozzle pressure ratio and free-stream Mach number on ejector gross-force ratio and pumping characteristics.

[redacted]

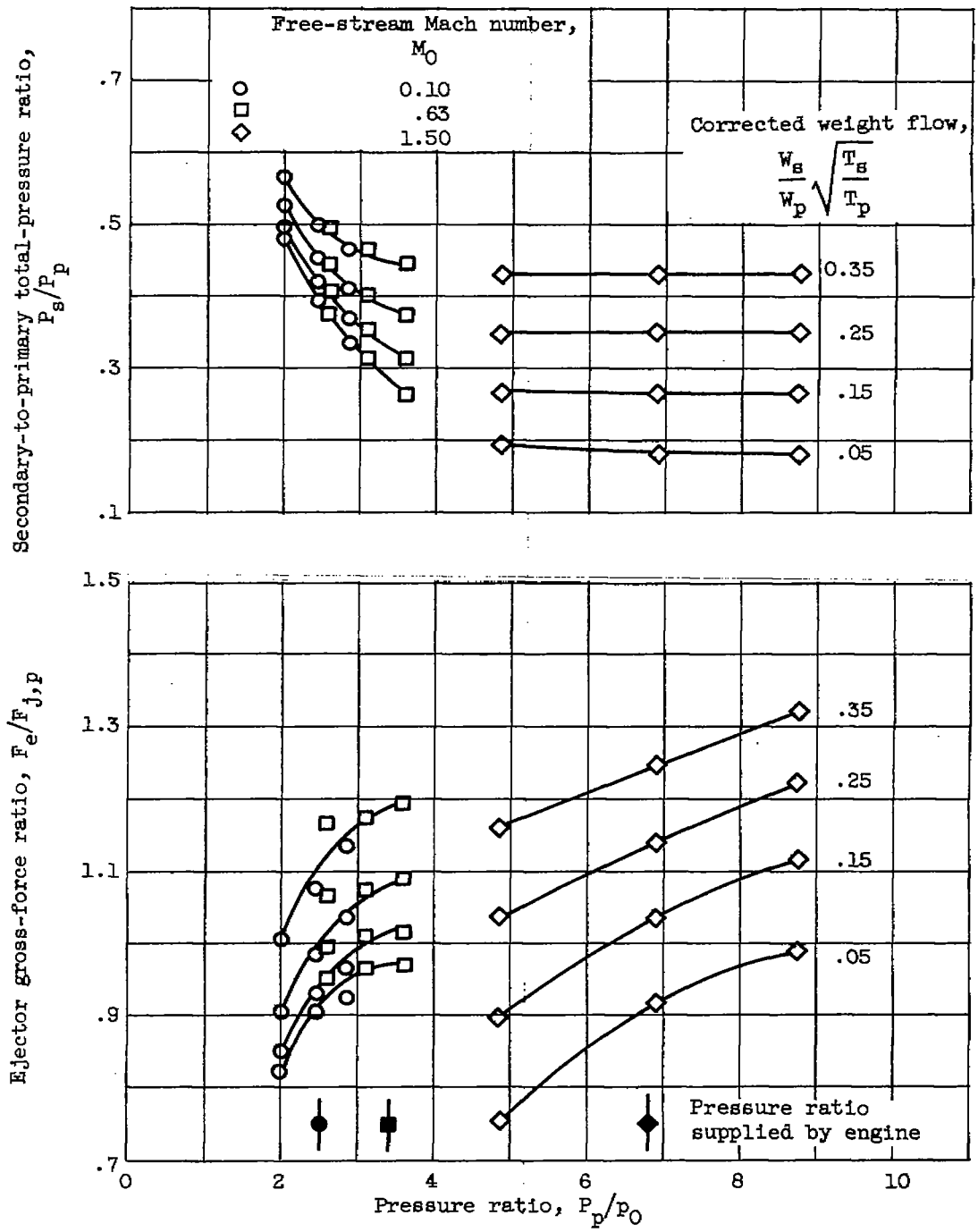

(b) Ejector 1.54-1.11.

Figure 6. - Continued. Effect of primary-nozzle pressure ratio and free-stream Mach number on ejector gross-force ratio and pumping characteristics.

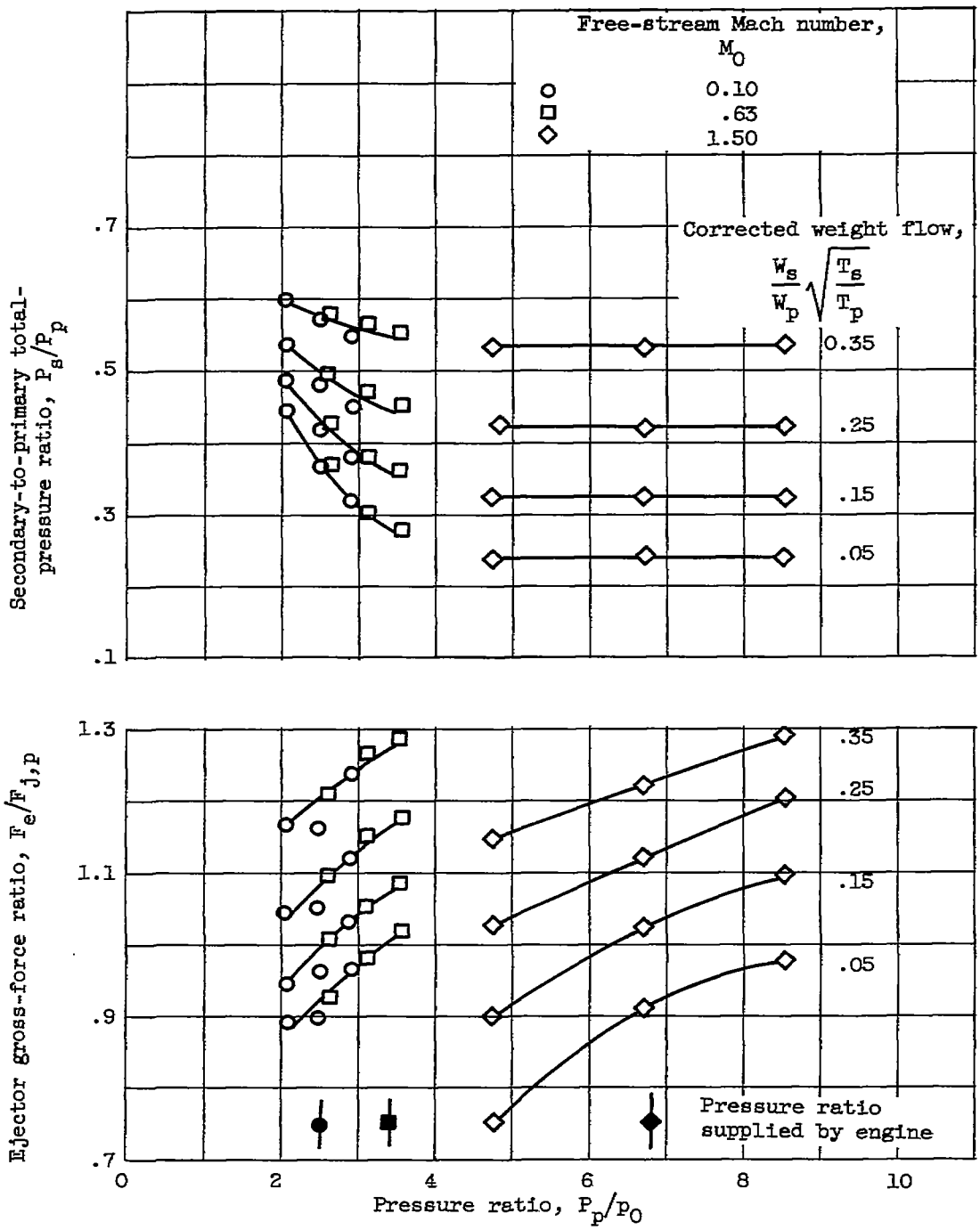

(c) Ejector 1.35-1.11SI.

Figure 6. - Continued. Effect of primary-nozzle pressure ratio and free-stream Mach number on ejector gross-force ratio and pumping characteristics.

[redacted]

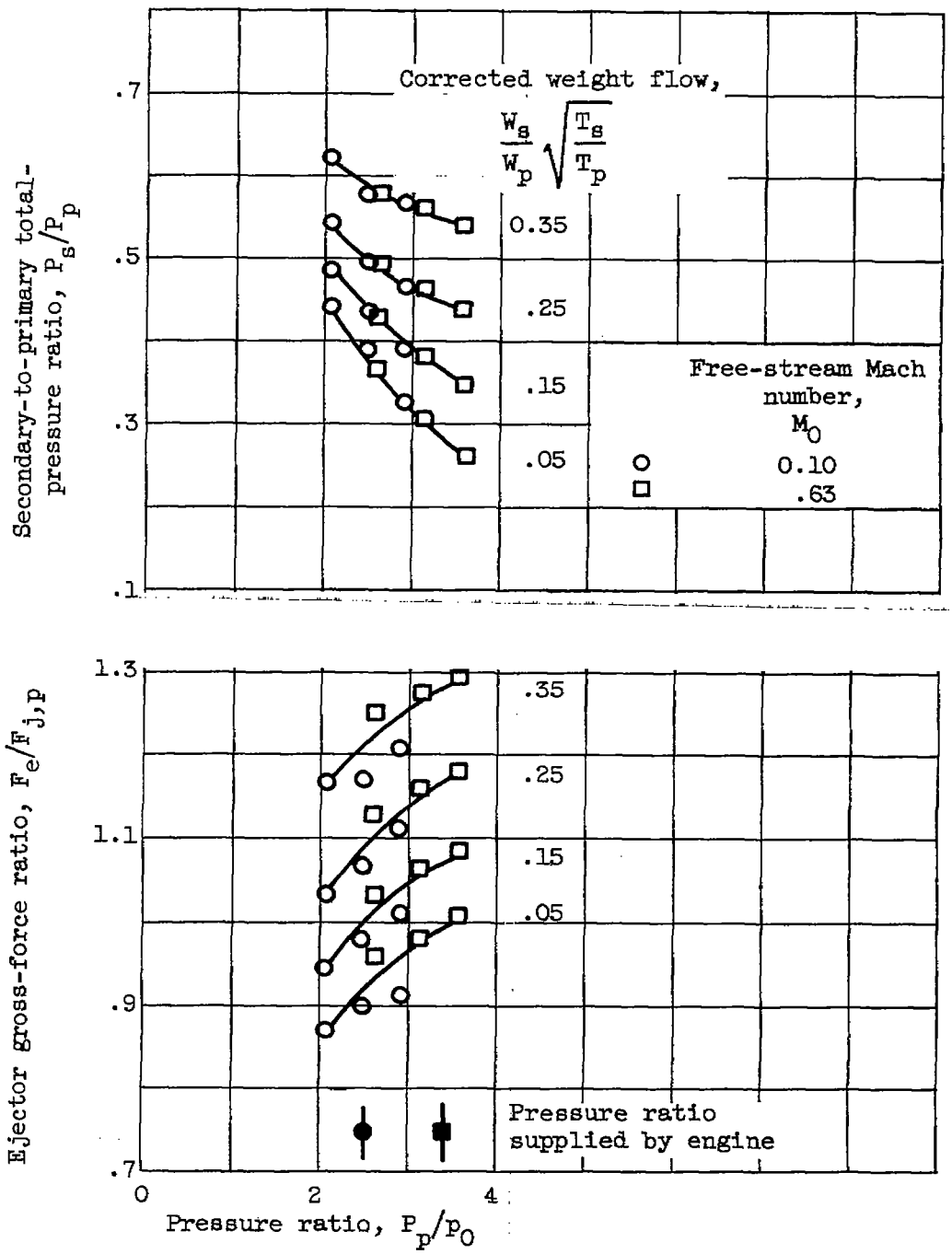

(d) Ejector 1.35-1.07I.

Figure 6. - Continued. Effect of primary-nozzle pressure ratio and free-stream Mach number on ejector gross-force ratio and pumping characteristics.

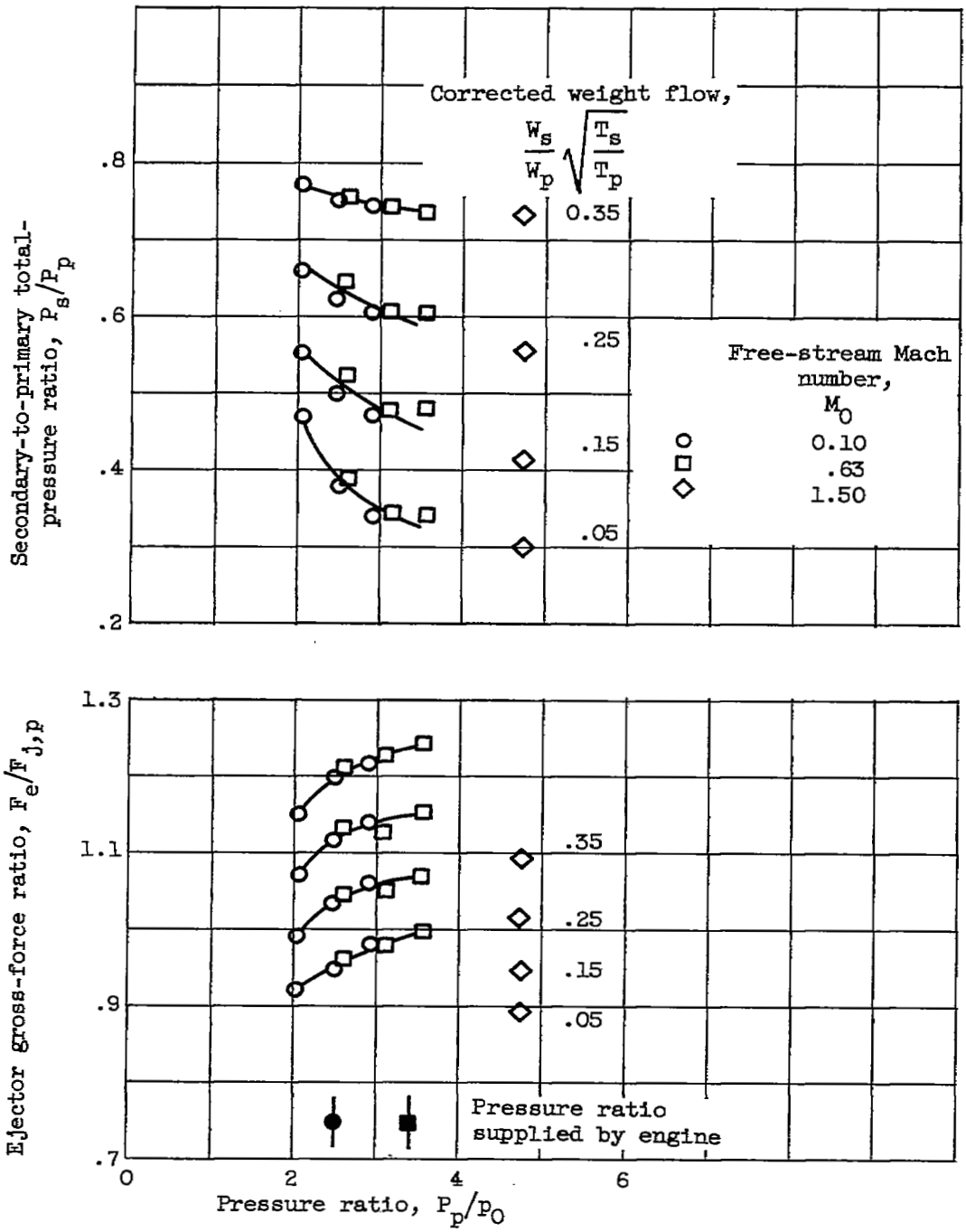

(e) Ejector 1.17-1.11SI.

Figure 6. - Continued. Effect of primary-nozzle pressure ratio and free-stream Mach number on ejector gross-force ratio and pumping characteristics.

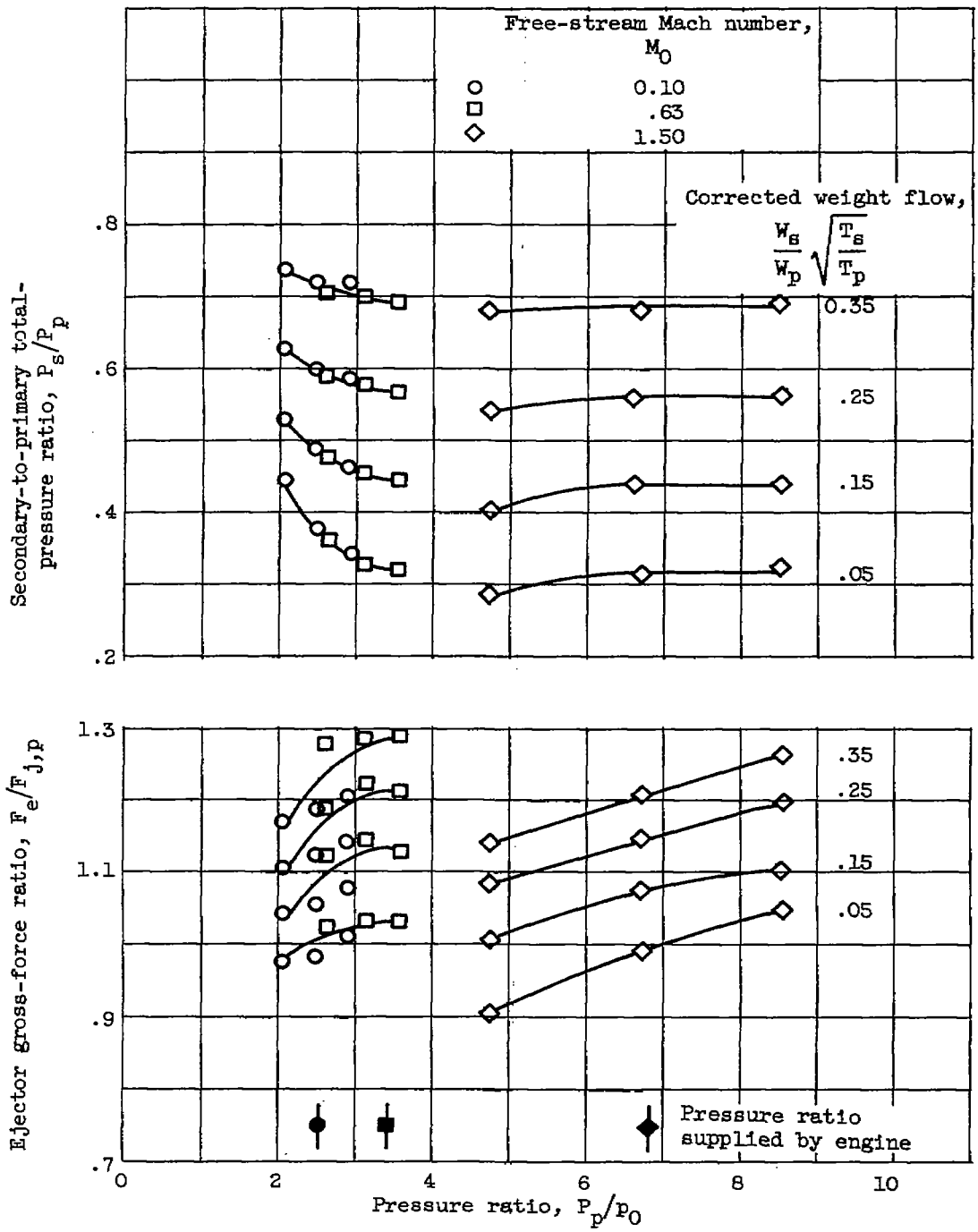

(f) Ejector 1.17-1.00I.

Figure 6. - Concluded. Effect of primary-nozzle pressure ratio and free-stream Mach number on ejector gross-force ratio and pumping characteristics.

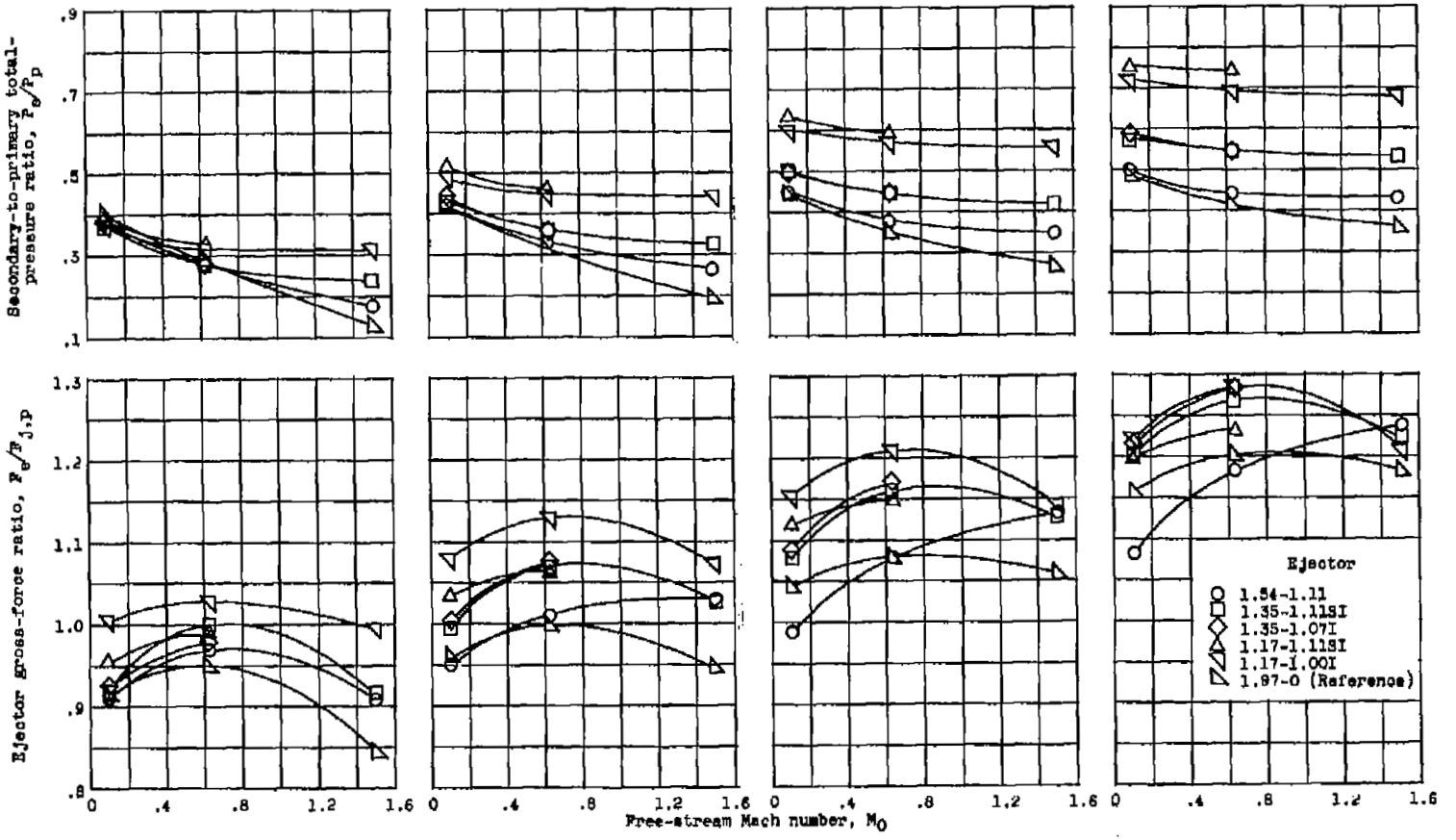

(a) Corrected weight-flow ratio, 0.08.

(b) Corrected weight-flow ratio, 0.15.

(c) Corrected weight-flow ratio, 0.25.

(d) Corrected weight-flow ratio, 0.35.

Figure 7. - Comparison of ejector gross-force and pumping performance at nozzle pressure ratios supplied by typical turbojet engine.

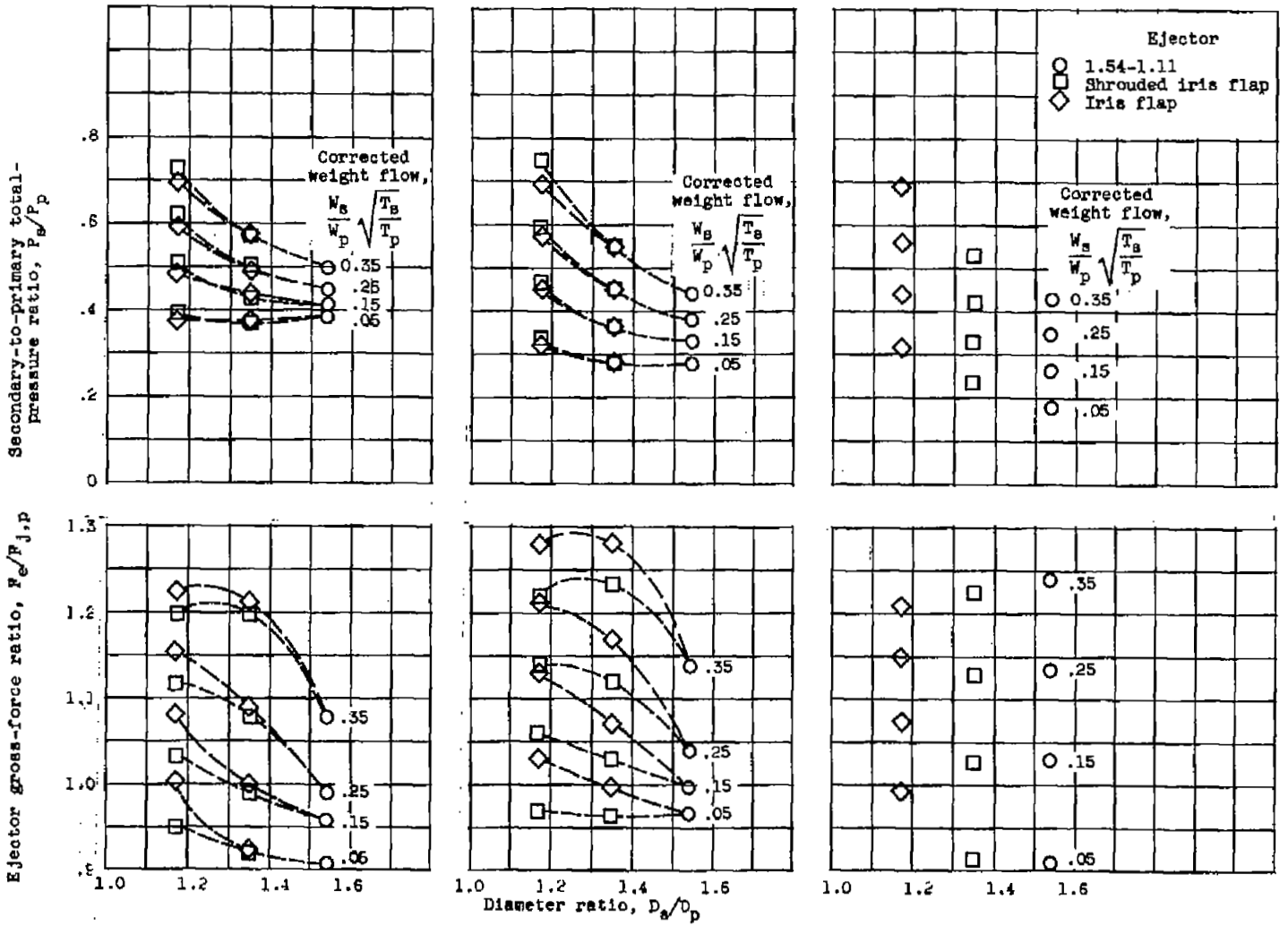

(a) Pressure ratio, 2.5; free-stream Mach number, 0.10.

(b) Pressure ratio, 3.4; free-stream Mach number, 0.63.

(c) Pressure ratio, 6.8; free-stream Mach number, 1.50.

Figure 8. - Effect of varying diameter ratio by iris flaps on ejector performance.

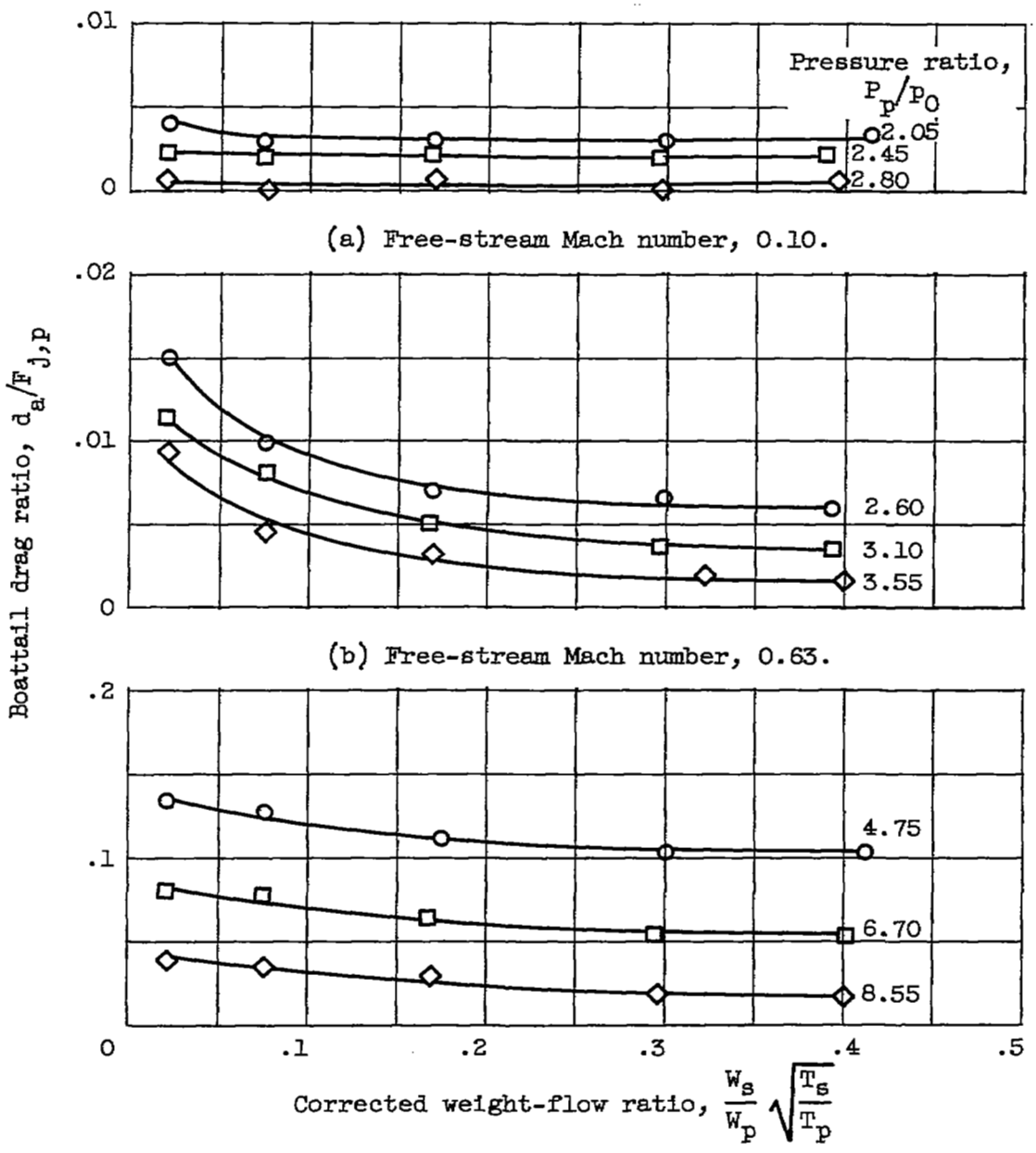

Figure 9. - Effect of primary-nozzle pressure ratio and free-stream Mach number on boattail drag of ejector 1.35-1.11SI.

[redacted]

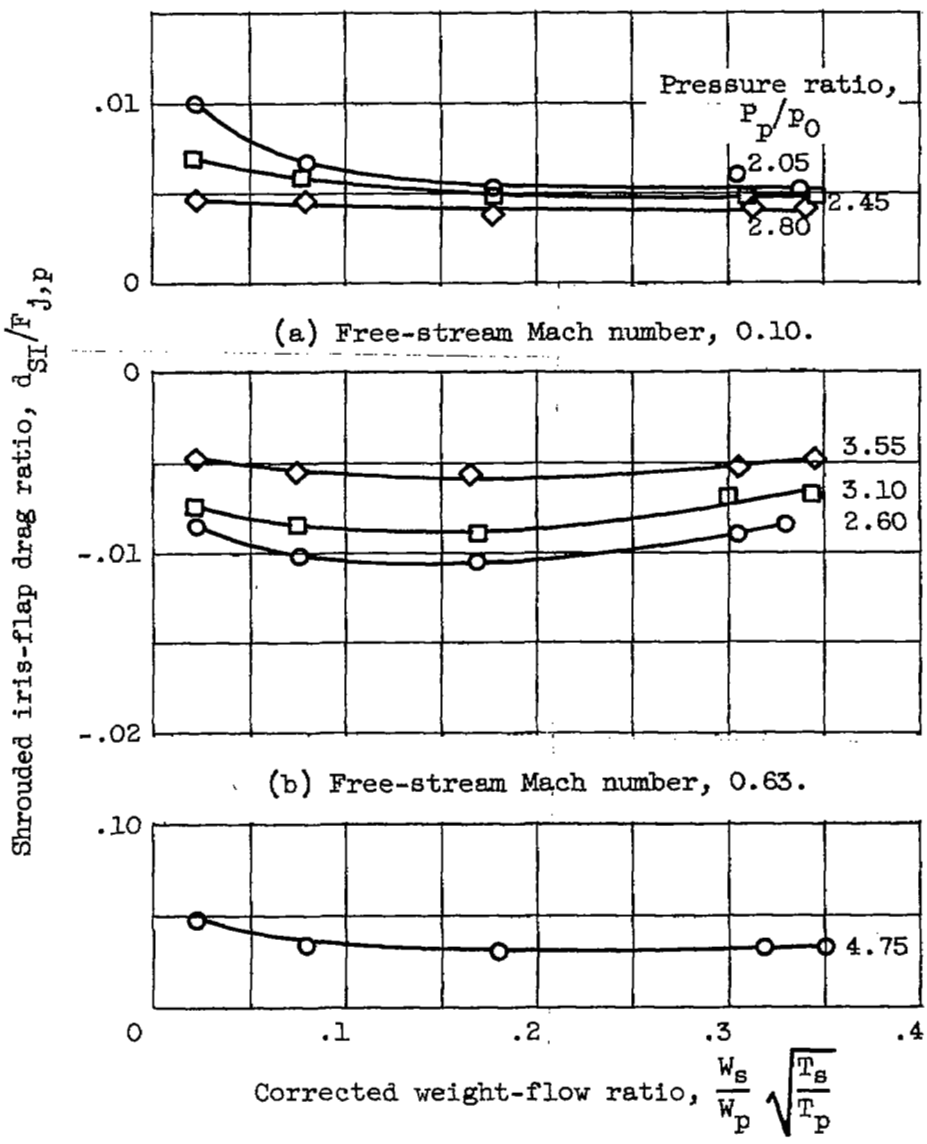

Figure 10. - Effect of primary-nozzle pressure ratio and free-stream Mach number on drag of shrouded iris flap of ejector 1.17-1.11SI.

NACA-Langley - 4-21-55 - 350